frontiers in Materials

ORIGINAL RESEARCH
published: 07 September 2021
doi: 10.3389/fmats.2021.728898

Corrosion Behavior and Passive Film Composition of Alloy 825 in High Temperature and High H_2S-CO_2 Containing Environment

Zhe Feng[1], Xuehua Fan[2], Zhu Wang[1], Yong Yu[2], Lijuan Chen[2], Yanxia Du[1] and Lei Dong[2]*

[1]Institute for Advanced Materials and Technology, University of Science and Technology Beijing, Beijing, China, [2]China Petroleum Engineering and Construction Co., Ltd. Beijing Company, Beijing, China

The effect of high temperature on corrosion behavior and passive film composition of Ni-based alloy 825 in H_2S-containing environment was investigated by Confocal Laser Microscope (CLM), Scanning Electron Microscope (SEM), Energy Dispersive Spectrometer (EDS), and X-ray Photoelectron Spectroscopy (XPS). The experiment was carried out at 150 and 230°C in NaCl solution. The partial pressure of H_2S was set to 1.2 MPa and CO_2 was set to 3.2 MPa. The results showed that Ni-based alloy 825 presented good general corrosion resistance. Pitting corrosion was likely to occur at 230°C because of Cr depleted in the passive film. NiS appeared at high temperature and is damaging to protectiveness of passive film.

Keywords: nickel based alloy, hydrogen sulfide, pitting, passive film, high temperature

OPEN ACCESS

Edited by:
Chong Sun,
China University of Petroleum, China

Reviewed by:
Jiankuan Li,
University of Alberta, Canada
Yong Xiang,
China University of Petroleum, China

****Correspondence:***
Zhu Wang
wangzhu1303@126.com

Specialty section:
This article was submitted to Environmental Degradation of Materials, a section of the journal Frontiers in Materials

Received: *22 June 2021*
Accepted: *28 July 2021*
Published: *07 September 2021*

Citation:
Feng Z, Fan X, Wang Z, Yu Y, Chen L, Du Y and Dong L (2021) Corrosion Behavior and Passive Film Composition of Alloy 825 in High Temperature and High H_2S-CO_2 Containing Environment. Front. Mater. 8:728898. doi: 10.3389/fmats.2021.728898

INTRODUCTION

With the increase in energy demand and development in oil field exploitation methods, ultra-deep oil and gas fields have gradually increased. During cooperation with colleagues in field, we found the environment in working condition is more severe than expected. As depth increases, downhole equipment is facing temperatures above 100°C. Because of the high H_2S, high Cl^-, and high CO_2 that exist in the downhole environment, materials usually used in production suffer from decreasing corrosion resistance. Carbon steel will face high corrosion risk in the harsh corrosive environment (Javidi and Bekhrad, 2018). Nickel-based alloys with better corrosion resistance are used in production equipment. There was plenty of research about the corrosion behavior at temperature lower than 200°C. H_2S partial pressure was stabilized at several KPa. This didn't match to the high temperature and high H_2S partial pressure in production. There are few reports on the passive film composition of alloy 825 under extreme environments. The relation between passive film composition and corrosion resistance still needs to be studied. Incoloy 825 is the most widely used Ni-based alloy in engineering. Its high content of Cr and Ni makes for great passivation performance and good corrosion resistance. Early research had discovered the passivation ability of Cr (Kirchheim et al., 1989) and it became a common element in various stainless steels. Mo is a typical additive to improve the stability of passive film and prevent occurrence of localized corrosion (Laszczyńska et al., 2017; Hendersona et al., 2018).

However, Ni-based alloys cannot be corrosion-free in extreme environments. There were many researchers in related fields. Elshawesh et al. (2015) had reported a failure case of a 825 joint in CO_2/H_2S environment at 60°C which was caused by pitting corrosion in long-term service. Banaś et al. (2007) presented S^{2-} ion could hinder the formation of oxide film and changed the corrosion mechanism of alloys. Ding et al. (2014) believed H_2S accelerate the anodic and cathodic reactions of stainless steel. H_2S could reduce the corrosion resistance of materials by changing the electrochemical properties of passive

TABLE 1 | The chemical composition of 825 (wt%).

Alloy	C	Cr	Mn	Si	Cu	Mo	S	Al	Ti	Fe	Ni
825	0.01	21.3	0.45	0.18	2.24	3.08	0.003	0.21	0.75	30	bal

film. Alexander et al. (2018) compared the difference of corrosion mechanism between duplex stainless steel and nickel-based alloy in H_2S environment. Both materials showed the susceptibility of selective corrosion. Dong et al. (2011) revealed the increase of austenite phase could increase the corrosion resistance of crevice corrosion. Cheng et al. (2000) proved the presence of nickel sulfide and H_2S accelerated the corrosion rate of Alloy 825 by using an electrochemistry method. Temperature can influence the corrosion resistance of materials. Zhao et al. (2011) tested Ni-based alloy using a solution containing H_2S/CO_2 and found the increase in temperature resulted in a higher corrosion rate while presence of elemental sulfur led to localized corrosion. Elizabeth et al. (2014) used optical measurement to observe corrosion behavior 825 in 3 M NaCl with CO_2 at 250°C. However, the downhole environment is much more severe. The Cl^- concentration is nearly saturated under severe working conditions and the H_2S and CO_2 could reach MPa level. Further research on Ni-based alloy corrosion behavior under severe conditions is still needed.

In this paper, the corrosion resistance of the passive film of Ni-based alloys has been further studied by using Confocal Laser Microscope (CLM), Scanning Electron Microscope (SEM), Energy Dispersive Spectrometer (EDS), and X-ray photoelectron spectroscopy (XPS). The pitting corrosion behavior of Alloy 825 by changing the temperature in a high Cl^- high H_2S/CO_2 environment is discussed.

MATERIALS AND METHODS

Materials and Solutions

All test specimens were cut from an 825 Ni-based Alloy plate. The chemical composition of 825 is listed in **Table 1**.

The corrosion test specimens were cut to 40 mm × 20 mm × 3 mm. The specimens for surface characterization were cut to 10 mm × 10 mm × 3 mm in size. All samples were cleaned with acetone, alcohol, and deionized water after machining. Corrosion test specimens were polished to 600# and surface characterization specimens were successively polished to 2000# to make it suitable for SEM and XPS test. Specimens were cleaned by deionized water and alcohol, then dried by cool air, and then weighed.

For a more precise simulation of working condition, 350 g L^{-1} NaCl was applied in an immersion test. The test solution containing approximately 350 g L^{-1} NaCl were purged with N_2 for 2 h. Before the test, solution was saturated with CO_2 and then H_2S was introduced and stabilized at 1.2 MPa. The partial pressure of CO_2 is controlled to 3.2 MPa which is similar to working condition. As the gas pressure is fully stabilized, the autoclaves were heated to 150 and 230°C, respectively. The test duration was set to be 720 h. The total pressure of two conditions is about 5 MPa after heating.

Weight Loss

After experiment, specimens were taken out of the autoclave. Deionized water and acetone were used to rinse. The specimens were blow-dried by cool wind. The corrosion product was removed by 15% HCl and then weighed. The corrosion rate was calculated by the following equation:

$$CR = \frac{87600W}{A \times t \times \mathrm{D}} \quad (1)$$

where CR is the corrosion rate (mm/a), W is for total weight loss (g), A is for sample surface area (cm^3), t is for experiment time (s), D is for density which is 8.14 g/cm^3 for Alloy 825.

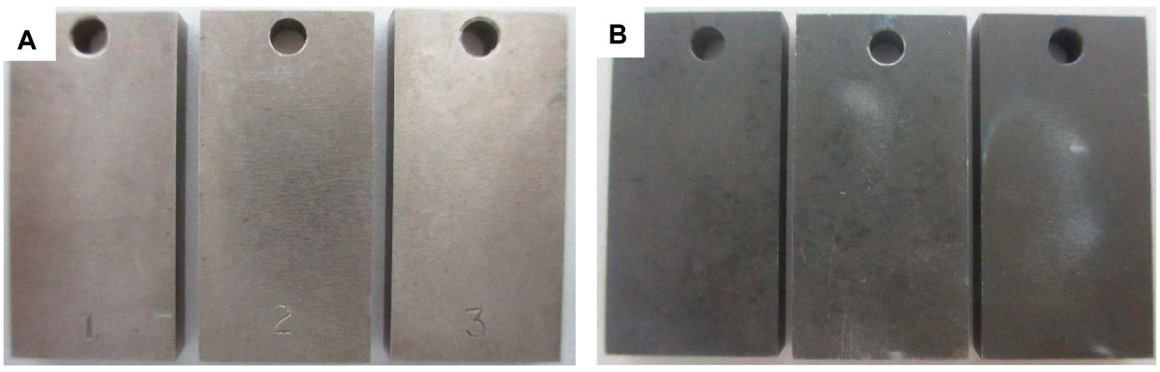

FIGURE 1 | Macro-morphology of 825 sample after the immersion tests at different temperatures: **(A)** no obvious corrosion product at 150°C, **(B)** black corrosion product at 230°C.

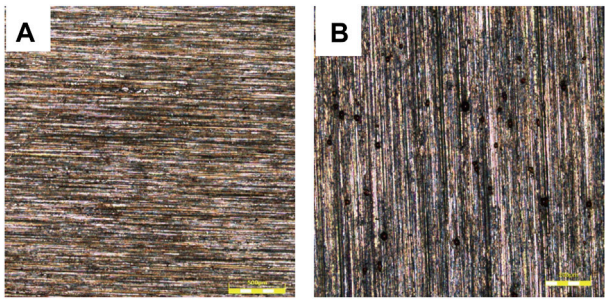

FIGURE 2 | Micro-morphology of 825 sample after the immersion tests at different temperatures without remove corrosion products: **(A)** no pit observed at 150°C. **(B)** black pits founded at 230°C.

Surface Morphology

CLM and SEM were used to observe the corrosion product on the specimen. After the immersion test, the specimens were rinsed with deionized water and dried by cool air. The surface of the specimens was analyzed using CLM to obtain the dimensional information of pits. A Quanta250 environmental SEM equipped with an EDS was used to analyzed the surface morphology and corrosion products. The depth of corrosion pits was acquired and pitting corrosion rate was calculated by the following equation:

$$CR_p = \frac{8760D}{t} \quad (2)$$

where CR_P is the pitting corrosion rate (mm/a), D is for depth of the deepest pits (mm), and t is for experiment time (h).

Surface Characterization

The composition of the passive films formed at various temperatures was analyzed by XPS with a PHI5000 VersaProbe III [monochromatic Al Kα (hυ = 1,486.6 eV), analysis angle 45°]. The shift change was adjusted by C 1s at 284.8 eV. XPSPEAK 41 was used to analyzed the XPS result.

RESULT

Corrosion Rate

We used **Eq. 1** to calculate the general corrosion rate. The corrosion rate is 0.0007 ± 0.0001 mm/a for 150°C and 0.0010 ± 0.0001 mm/a for 230°C. The Alloy suffered from higher general corrosion rate at 230°C than 150°C. However, it should be pointed out that corrosion rates were extremely low, indicating Alloy 825 showed good general corrosion resistance under the testing conditions.

Surface Morphology

Figure 1 shows the morphology of Alloy 825 samples after the immersion tests at different temperatures. It was observed that samples lost metallic luster after test.

Figure 2 shows the micro-morphology of the 825 sample after the immersion tests at different temperatures. There is no obvious pit on the surface of the sample tested at 150°C. A large number of pits were found at 230°C. Several researches (Banaś et al., 2007; Tomio et al., 2015) indicated that in H_2S-containing environments the Ni-Cr-Mo alloy would form oxides of Cr and Mo and black sulfides such as FeS, NiS, and MoS_2 on the surface. The composition of passive film is different from that formed in H_2S-free environment (Wang et al., 2017; Wang et al., 2018; Wang et al., 2020).

Figure 3 shows micro-morphology of the 825 sample after removal of the corrosion products. The corrosion product was removed with 15% HCl. The samples tested at 150°C showed no pit on the surface, and no height difference caused by corrosion was observed on the entire surface. A large number of pits could be clearly found on the surface of the specimen and were evenly distributed on the surface at 230°C. The depth of pits ranged from 7 to 10 μm. The pitting corrosion rate was 0.12 mm/a according to **Eq. 2**. The rising temperature greatly increased localized corrosion susceptibility of Alloy 825 in a sulfur-containing environment.

Figure 4 shows the SEM images of Alloy 825 sample after the immersion tests. A layer of film could be observed on the surface of the sample tested in 3.2 MPa CO_2, 1.2 MPa H_2S at 150°C. The film was intact and had no obvious corrosion product accumulation. The

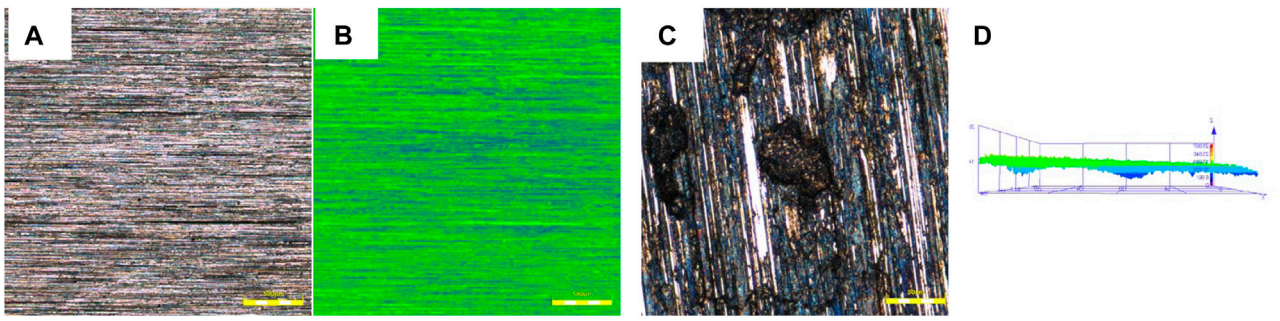

FIGURE 3 | Micro-morphology of 825 sample after removal of the corrosion products at different temperatures: **(A, B)** no pit founded at 150°C. **(C, D)** black pits founded at 230°C and scanned by CLM.

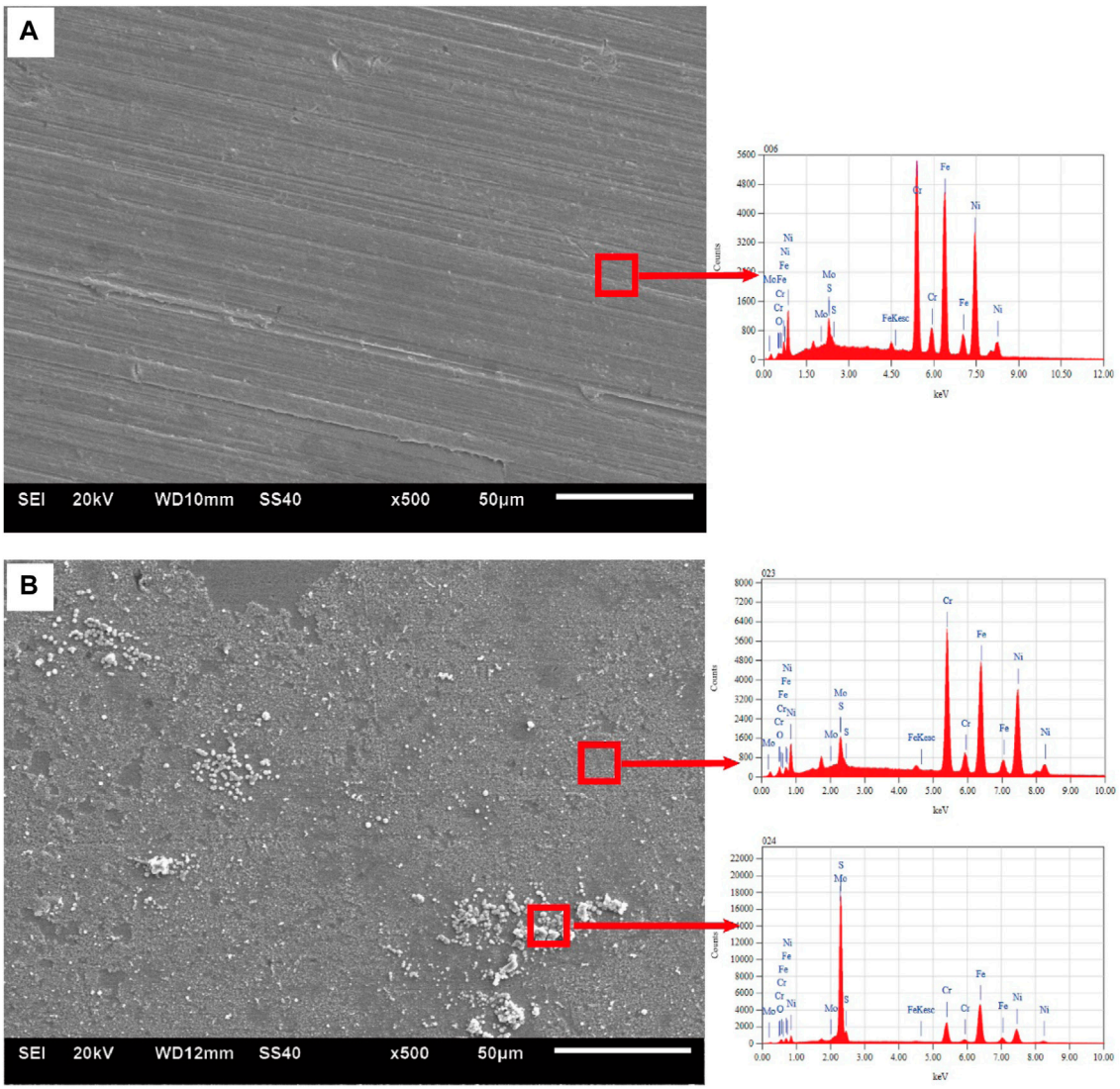

FIGURE 4 | SEM and EDS result of Alloy 825: **(A)** no obvious corrosion products at 150°C **(B)** particle corrosion products observed at 230°C.

material showed good corrosion resistance in this environment. The particles corrosion product appeared at 230°C, indicating the corrosion tendency at 230°C is higher than that at 150°C. Scratches still could be seen over the surface, which suggested the material had strong resistance to general corrosion. This is consistent with the results in *Corrosion Rate*. EDS was used to analyze the surface corrosion product film. The analysis found corrosion product film contains a small amount of sulfur element and the sulfur content in the particle corrosion product is much greater than corrosion product film.

XPS Result

For corrosion product deposited on the corrosion product film and the corrosion product film, XPS is used for composition analysis. All samples were sputtered for 30 s to remove the outermost product film. The sampling depth of XPS is 0.5–2 nm for metals and about 1–3 nm for inorganic products.

Figure 5 shows the result of XPS results at 150°C. It mainly contained Cr, Fe, Ni, Mo, and O and S. The Cr shows obvious split peaks. The peaks were corresponding to Cr_2O_3 (576.8 eV) and CrO_3 (578.5 eV). Cr oxides were still formed in high-temperature H_2S-containing environment which was the main reason for Alloy 825 to maintain good corrosion performance under severe conditions. Fe spectrum were mainly composed of Fe_2O_3 (710.9 eV) and FeS (713.8 eV). It can be determined the corrosion products are Fe^{2+}/Fe^{3+} oxides and sulfides in the passive film. The content of Mo in the passive film is the least of the four elements. Its spectrum was split into three peaks of Mo, MoS_2, and MoO_3. The Ni spectrum mainly consisted of $Ni(OH)_2$ (861.2 eV) and satellites. O spectrum was divided into O^{2-}(530.2 eV) and OH^-(531.6 eV). The peak of S was mainly S^{2-}(530.2 eV).

Figure 6 shows the surface XPS results at 230°C, 1.2 MPa H_2S, 3.2 MPa CO_2. The Cr and Fe spectra could be separated to similar

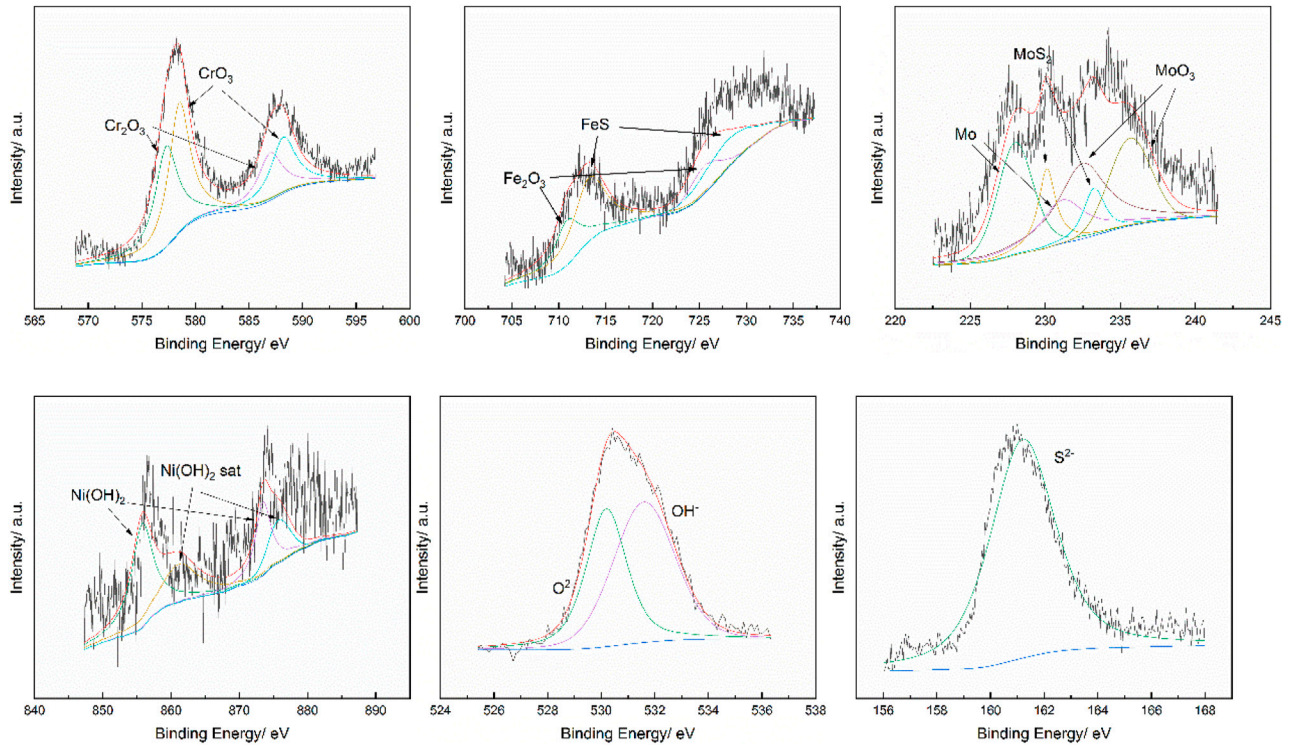

FIGURE 5 | XPS analysis results for Alloy 825 at 150°C, 1.2 MPa H_2S 3.2 MPa CO_2.

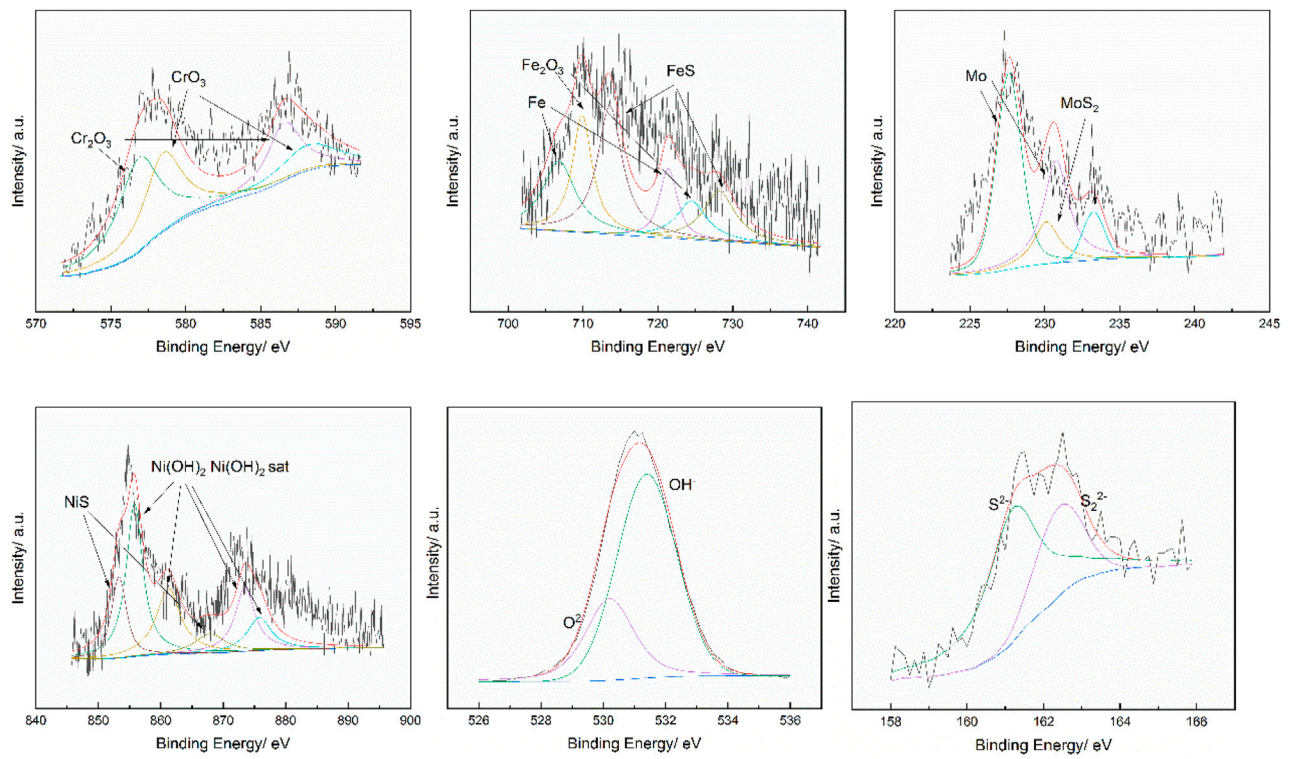

FIGURE 6 | XPS analysis results for Alloy 825 at 230°C, 1.2 MPa H_2S 3.2 MPa CO_2.

peak as 150°C. There were Mo and MoS_2 in the Mo spectrum. However, MoO_3 disappeared at 230°C.

Ni formed NiS and $Ni(OH)_2$ at 230°C. The appearance of sulfides in the passive film lead to a decrease in general corrosion resistance and induced pitting corrosion. The O spectrum was composed by O^{2-} and OH^- which is the same as the result at 150°C. The S spectrum could be separated to different peaks of S^{2-} and S_2^{2-}.

Figure 7 shows the relative proportions of the elements in the passive film under the two conditions. As the temperature increased, the content of Cr in the passive film reduced. At 150°C, the relative proportion of Cr was above 60%, which reduced to 20% after the temperature was increased to 230°C. At the same time, the relative proportions of Fe and Ni increased. At 150°C, the relative ratios of Fe and Ni in passive film were lower than that of Cr which was less than 15%. However, when the temperature raised to 230°C, the relative ratio was increased to about 30% for Fe and 40% for Ni. Mo kept about 10% in both conditions.

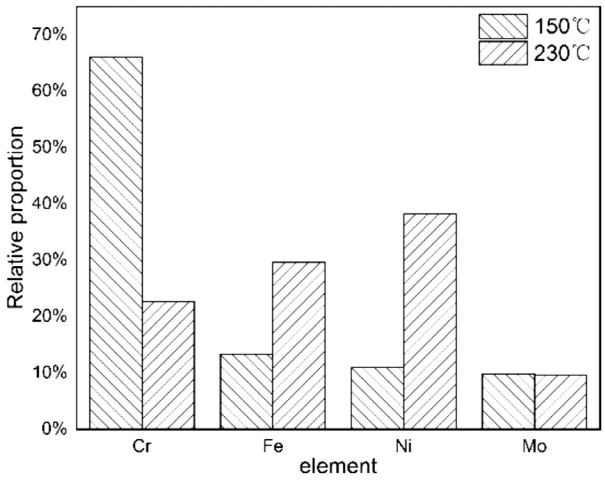

FIGURE 7 | The comparison of relative proportions of the elements in passive film of Alloy 825 under two conditions.

DISCUSSION

The increase in temperature influenced the corrosion behavior of nickel-based alloys in H_2S-containing environments. It increased the corrosion rate and risk of pitting corrosion by affecting the composition of the passive film. From 150°C to 230°C, changes occurred in the composition of the surface passive film of nickel-based Alloy 825. Under sulfur-containing conditions, S appeared in the passive film and sulfide had detrimental effect to isolated corrosive media.

At 150°C, the content of Cr in the passive film was higher than that of Alloy 825 which showing enrichment in passive film. When temperature increased, the Cr in the passive film greatly reduced. This is consistent with other studies at lower temperatures which pointed out an increasing loss of Cr_2O_3 as temperature increases (Zhang and Shoesmith, 2013).

The oxides and sulfides of Fe were formed in both conditions. The content of Fe in the passive film increases with temperature. Low corrosion resistance of Fe/FeS results in an increase in the dissolution rate at 230°C.

At lower temperatures, Ni only formed the $Ni(OH)_2$, while NiS was produced at high temperatures. Monnot (Monnot et al., 2017) found that appearance of sulfide will not only reduce the density of the film but also cause changes in the electrochemical property of passive film. The original ion-selective oxide film converted to the sulfide film which was lacking in ion-selective. This promoted the permeation of corrosive ions such as Cl^-, S^{2-}, and $CO_3{}^2$ to the base metal, increasing the pitting susceptibility. Therefore, pitting corrosion occurred in 825 at 230°C.

$Ni(OH)_2$ has good corrosion resistance. At the same time, the relative content of Ni in the passive film was significantly increased, which is close to the proportion of Ni in Alloy 825. Because of the formation of sulfides, the composition of the passive film changes and the corrosion resistance is reduced. The cathodic reaction of H_2S corrosion is a series of depolarization processes of H_2S, HS^-, and H^+. It lowers the pH of the environment as in the following:

$$H_2S + e^- \rightarrow H + HS^- \quad (3)$$

$$HS^- + e^- \rightarrow H + S^{2-} \quad (4)$$

The dissolution process of Ni at lower temperature is as following (Cheng et al., 2000):

$$Ni + H_2S + H_2O \rightarrow Ni(HS)_{ads} + H_3O^+ + e^- \quad (5)$$

$$Ni(HS)_{ads} \rightarrow NiHS^+ + e^- \quad (6)$$

$$NiHS^+ + H_3O^+ \Leftrightarrow Ni^{2+} + H_2S + H_2O \quad (7)$$

The hydrolysis reactions of Ni^{2+} lead to a formation of $Ni(OH)_2$ at 150°C.

At 230°C, Ni forms NiS in the sulfur-containing environment. NiS was a common corrosion product of nickel-based alloys after localized corrosion (Zhao et al., 2011). The NiS is formed as follows (Banaś et al., 2007; Sun et al., 2019; Li et al., 2021):

$$Ni + H_2S(aq) \rightarrow NiS + H_2 \quad (8)$$

NiS could not form a protective layer at low pH (Davoodi et al., 2011) which caused continuous corrosion. The presence of NiS may be one of the reasons for the decreased protection of passivation film at high temperature.

The content of Mo in the Alloy 825 is relatively low. But it plays a critical role in improving performance of the passive film. The sulfide and oxide of Mo have a good insulation of corrosion environment. Previous studies have shown that oxides of Mo have good corrosion resistance (Tomio et al., 2015; Henderson et al., 2019). Its protective performance comes from the ability to form passive film with cation selectivity. But when the temperature reaches 230°C, the following reaction may happen (Li et al., 2020a):

$$MoO_3 + 2HS^- \rightarrow MoS_2 + 2OH^- + H_2 \quad (9)$$

The reaction (9) is nearly impossible at room temperature and atmospheric pressure (Natishan et al., 1999). But

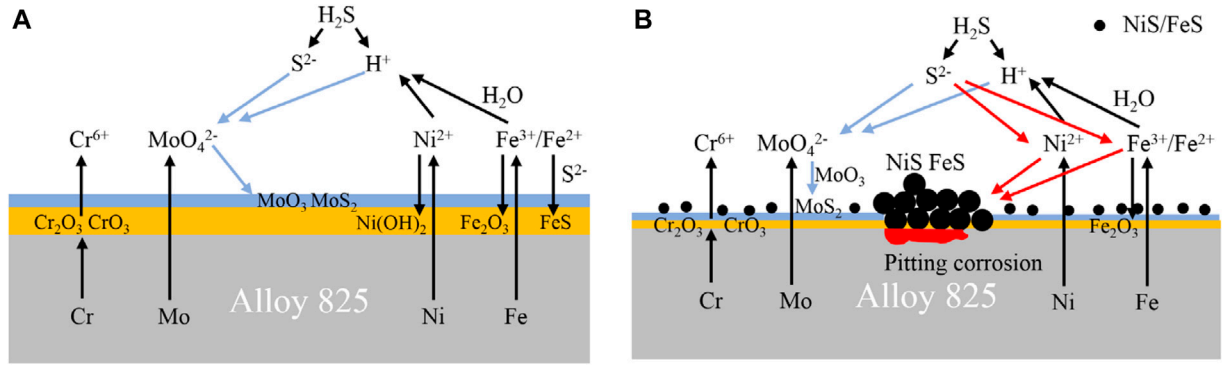

FIGURE 8 | The possible corrosion mechanism of Alloy 825 **(A)** 150°C **(B)** 230°C.

MoS_2 might formed in a sulfur-containing environment at 230°C.

Figure 8 shows the possible mechanism of Alloy 825 in the experimental environment. The corrosion behavior of passive film at lower temperature has been studied extensively (Zhang and Shoesmith, 2013; Henderson et al., 2019; JianqiaoYang et al., 2020; Li et al., 2020b; Nimmervoll et al., 2021). As **Figure 8A** shows, Mo is enriched in the outer layer and Ni/Cr in the metal border. This is the result of dissolution of passive film and the deposition of Mo oxide at low pH. NiS does not form and amount of FeS is limited. Dissolution/formation of passive film is relatively slow. Therefore, a complete oxide passive film can be formed to keep good corrosion resistance. With the increase of temperature, the dissolution/formation process of the passive film is accelerated. Because of the higher diffusion ability of Ni than Cr, it takes priority to combine with S^{2-} (Zhao et al., 2011), so NiS corrosion products are formed on the metal surface. MoO_3 is converted to MoS_2 with less corrosion resistance. The content of Cr is decreased in passive film. The surface was adhered by a loose layer of NiS/FeS and Mo sulfide without precipitating a protective film on the metal. When corrosive solution reaches substrate, pitting corrosion happens.

In summary, the increase in temperature will cause the corrosion of Alloy 825 to accelerate in high H_2S environment. At 150°C, Cr enriched passive film could still be formed on the surface of Alloy 825. There was only a small amount of FeS in the passive film, which had little effect on the corrosion resistance. The main composition of passive film was still Cr and Ni oxides. Oxides of Mo also provided great corrosion resistance. After the temperature rose to 230°C, the relative proportion of Cr in the passive film reduced while the proportion of Ni and Fe increased. The appearance of sulfide reduced the protectiveness of the passive film. Therefore, the surface of the sample tested at 150°C has only a thin film of corrosion products. No partial corrosion products were attached to the film and no obvious localized corrosion phenomenon was on the surface. On the surface of the specimen at 230°C, the performance of the passive film deteriorated and the corrosion rate increased. A thicker corrosion product layer appeared and partial corrosion product was attached to the surface. With defects in the passive film, pitting corrosion occurred.

CONCLUSION

In the present work, the corrosion behavior of Alloy 825 in high temperature with CO_2/H_2S and composition of passive film were studied. Weight loss, CLM, SEM, EDS, and XPS were used to analyze the specimen.

The conclusion is listed as follows:

1) The general corrosion of Alloy 825 is relatively slow in environment with 3.2 MPa CO_2, 1.2 MPa H_2S. Corrosion rate is 0.0007 ± 0.0001 mm/a for 150°C and 0.0010 ± 0.0001 mm/a for 230°C.
2) No pitting corrosion occurred at 150°C. When temperature raised to 230°C, pitting corrosion was likely to occur on the Alloy 825 surface.
3) The passive film is mainly composed of Cr_2O_3, CrO_3, Fe_2O_3, FeS, $Ni(OH)_2$, Mo, MoS at 150°C. At the higher temperature of 230°C, NiS is present in the passive film.
4) Cr suffered from a rapid decline in proportion while Fe and Ni were more enriched in film when temperature raised from 150°C to 230°C. NiS and MoS_2 also occur in film which caused the losses of corrosion resistance. Therefore, Alloy 825 faced risk of pitting corrosion in high temperature.

DATA AVAILABILITY STATEMENT

The original contributions presented in the study are included in the article/supplementary material, further inquiries can be directed to the corresponding author.

AUTHOR CONTRIBUTIONS

ZF finished the manuscript. He worked with XF and YY to analyze the results. ZW planned the scope of work. LC and LD conducted the immersion tests. YD revised the manuscript.

FUNDING

This work was supported by the Fundamental Research Funds for the Central Universities (FRF-TP-20-098A1) and National Natural Science Foundation of China (No. 51871027).

REFERENCES

Alexander, S., Moria, G., nigb, S. H., Weilc, M., Susanne, S., and Haubner, R. (2018). Comparison of the high-temperature chloride-induced corrosion between duplex steel and Ni based alloy in presence of H2S[J]. *Corrosion Sci.* 139, 76–82. doi:10.1016/j.corsci.2018.04.042

Banaś, J., Lelek-Borkowska, U., Mazurkiewicz, B., and Solarski, W. (2007). Effect of CO2 and H2S on the composition and stability of passive film on iron alloys in geothermal water[J]. *Electrochimica Acta* 52 (18), 5704–5714. doi:10.1016/j.electacta.2007.01.086

Cheng, X., Ma, H., Chen, S., Chen, X., and Yao, Z. (2000). Corrosion of nickel in acid solutions with hydrogen sulphide[J]. *Corrosion Sci.* 42 (2), 299–311. doi:10.1016/S0010-938X(99)00092-X

Davoodi, A., Pakshir, M., Babaiee, M., and Ebrahimi, G. R. (2011). A comparative H_2S corrosion study of 304L and 316L stainless steels in acidic media[J]. *Corrosion Sci.* 53, 399–408. doi:10.1016/j.corsci.2010.09.050

Ding, J., Zhang, L., Lu, M., Wang, J., Wen, Z., and Hao, W. (2014). The electrochemical behaviour of 316L austenitic stainless steel in Cl-containing environment under different H2S partial pressures[J]. *Appl. Surf. Sci.* 289, 33–41. doi:10.1016/j.apsusc.2013.10.080

Dong, H., Jiang, Y., Shi, C., Zhao, L., and Jin, L. (2011). Influence of the microstructure and alloying element on the polarization behaviour within the crevice of UNS S32304 duplex stainless steel[J]. *Corrosion Sci.* 53 (11), 3796–3804. doi:10.1016/j.corsci.2011.07.030

Elizabeth, Q. C., Jin, H., Posusta, R. S., Sharma, D. K., Yan, C., Guraieb, P., et al. (2014). Optical measurement of uniform and localized corrosion of C1018, SS 410, and Inconel 825 alloys using white light interferometry[J]. *Corrosion Sci.* 87, 383–391. doi:10.1016/j.corsci.2014.06.046

Elshawesh, F., Elhoud, A., Zeglam, W., Abusowa, K., and Mesalem, A. (2015). Corrosion Fatigue of Incoloy 825 Flare Gas Line Bellows of Expansion Joints[J]. *J. Fail. Anal. Prev.* 15 (1), 7–14. doi:10.1007/s11668-014-9900-9

Henderson, J. D., Li, X., Shoesmith, D. W., Noël, J. J., and Kevin, O. (2019). Molybdenum surface enrichment and release during transpassive dissolution of Ni-based alloys[J]. *Corrosion Sci.* 147, 32–40. doi:10.1016/j.corsci.2018.11.005

Hendersona, J. D., Ebrahimia, N., Dehnavia, V., Guo, M., Shoesmith, D. W., and Noël, J. J. (2018). The role of internal cathodic support during the crevice corrosion of Ni-Cr-Mo alloys[J]. *Electrochimica Acta* 283, 1600–1608. doi:10.1016/j.electacta.2018.07.048

Javidi, M., and Bekhrad, S. (2018). Failure analysis of a wet gas pipeline due to localised CO2 corrosion[J]. *Eng. Fail. Anal.* 89, 46–56. doi:10.1016/j.engfailanal.2018.03.006

JianqiaoYang, S. W., Li, Y., and Xu, D. (2020). Under-deposit corrosion of Ni-based alloy 825 and Fe-Ni based alloy 800 in supercritical water oxidation environment[J]. *Corrosion Sci.* 167, 108493. doi:10.1016/j.corsci.2020.108493

Kirchheim, R., Heine, B., Fischmeister, H., Hofmann, S., Knote, H., and Stolz, U. (1989). The passivity of iron-chromium alloys[J]. *Corrosion Sci.* 29 (7), 899–917. doi:10.1016/0010-938X(89)90060-7

Laszczyńska, A., Tylus, W., Winiarski, J., and Szczygieł, I. (2017). Evolution of corrosion resistance and passive film properties of Ni-Mo Alloy coatings during exposure to 0.5 M NaCl solution[J]. *Surf. Coat. Tech.* 317, 26–37. doi:10.1016/j.surfcoat.2017.03.043

Li, J., Sun, C., Roostaei, M., Mahmoudi, M., Fattahpour, V., Zeng, H., et al. (2020). Characterization and corrosion behavior of electroless Ni-Mo-P/Ni-P composite coating in CO_2/H_2S/Cl^- brine: Effects of Mo addition and heat treatment[J]. *Surf. Coat. Tech.* 403, 126416. doi:10.1016/j.surfcoat.2020.126416

Li, L., Wang, J., Xiao, J., Yan, J., Fan, H., sun, L., et al. (2021). Time-dependent corrosion behavior of electroless Ni-P coating in H_2S/Cl^- environment[J]. *Int. J. Hydrogen Energ.* 46 (21), 11849–11864. doi:10.1016/j.ijhydene.2021.01.053

Li, X., Henderson, J. D., Filice, F. P., Zagidulin, D., Biesinger, M. C., Sun, F., et al. (2020). The contribution of Cr and Mo to the passivation of Ni22Cr and Ni22Cr10Mo alloys in sulfuric acid[J]. *Corrosion Sci.* 176, 109015. doi:10.1016/j.corsci.2020.109015

Monnot, M., Nogueira, R. P., Roche, V., Berthomé, G., Chauveau, E., Estevezb, R., et al. (2017). Sulfide stress corrosion study of a super martensitic stainless steel in H_2S sour environments: Metallic sulfides formation and hydrogen embrittlement [J]. *Appl. Surf. Sci.* 394, 132–141. doi:10.1016/j.apsusc.2016.10.072

Natishan, P. M., Jones-Meehan, J., Loeb, G. I., Little, B. J., Ray, R., and Beard, M. (1999). Corrosion Behavior of Some Transition Metals and 4340 Steel Metals Exposed to Sulfate-Reducing Bacteria[J]. *Corrosion* 55, 1062–1068. doi:10.5006/1.3283943

Nimmervoll, M., Schmid, A., Mori, G., Honig, S., and Haubner, R. (2021). Surface sulphide formation on high-temperature corrosion resistant alloys in a H_2S-HCl-CO_2 mixed atmosphere[J]. *Corrosion Sci.* 181, 109241. doi:10.1016/j.corsci.2021.109241

Sun, C., Zeng, H., and Luo, J. (2019). Unraveling the effects of CO_2 and H_2S on the corrosion behavior of electroless Ni-P coating in CO_2/H_2S/Cl^- environments at high temperature and high pressure[J]. *Corrosion Sci.* 148, 317–330. doi:10.1016/j.corsci.2018.12.022

Tomio, A., MasayukiSagara, T. D., HisashiAmaya, N. O., and Kudo, T. (2015). Role of alloyed molybdenum on corrosion resistance of austenitic Ni-Cr-Mo-Fe alloys in H_2S-Cl-environments[J]. *Corrosion Sci.* 98, 391–398. doi:10.1016/j.corsci.2015.05.053

Wang, Z., Feng, Z., and Zhang, L. (2020). Effect of high temperature on the corrosion behavior and passive film composition of 316 L stainless steel in high H2S-containing environments[J]. *Corrosion Sci.* 174, 108844. doi:10.1016/j.corsci.2020.108844

Wang, Z., Zhang, L., Tang, X., and Minxu, L. (2017). The surface characterization and passive behavior of Type 316L stainless steel in H_2S-containing conditions[J]. *Appl. Surf. Sci.* 423, 457–464. doi:10.1016/j.apsusc.2018.07.12210.1016/j.apsusc.2017.06.214

Wang, Z., Zhang, L., Zhang, Z., and Minxu, L. (2018). Combined effect of pH and H2S on the structure of passive film formed on type 316L stainless steel[J]. *Appl. Surf. Sci.* 458, 686–699. doi:10.1016/j.apsusc.2018.07.122

Zhang, X., and Shoesmith, D. W. (2013). Influence of temperature on passive film properties on Ni-Cr-Mo Alloy C-2000[J]. *Corrosion Sci.* 76, 424–431. doi:10.1016/j.corsci.2013.07.016

Zhao, X. H., Han, Y., Bai, Z. Q., and Wei, B. (2011). The experiment research of corrosion behaviour about Ni-based alloys in simulant solution containing H2S/CO2[J]. *Electrochimica Acta* 56 (22), 7725–7731. doi:10.1016/j.electacta.2011.05.116

Conflict of Interest: Authors XF, YY, LC, and LD are employed by the China Petroleum Engineering and Construction Co., Ltd. Beijing Company.

The remaining authors declare that the research was conducted in the absence of any commercial or financial relationships that could be construed as a potential conflict of interest.

Publisher's Note: All claims expressed in this article are solely those of the authors and do not necessarily represent those of their affiliated organizations, or those of the publisher, the editors and the reviewers. Any product that may be evaluated in this article, or claim that may be made by its manufacturer, is not guaranteed or endorsed by the publisher.